nature materials

LETTERS

PUBLISHED ONLINE: 13 JANUARY 2013 | DOI: 10.1038/NMAT3537

Singular phase nano-optics in plasmonic metamaterials for label-free single-molecule detection

V. G. Kravets[1], F. Schedin[1], R. Jalil[1], L. Britnell[1], R. V. Gorbachev[1], D. Ansell[1], B. Thackray[1], K. S. Novoselov[1], A. K. Geim[1], A. V. Kabashin[2]* and A. N. Grigorenko[1]*

The non-trivial behaviour of phase is crucial for many important physical phenomena, such as, for example, the Aharonov–Bohm effect[1] and the Berry phase[2]. By manipulating the phase of light one can create 'twisted' photons[3,4], vortex knots[5] and dislocations[6] which has led to the emergence of the field of singular optics relying on abrupt phase changes[7]. Here we demonstrate the feasibility of singular visible-light nano-optics which exploits the benefits of both plasmonic field enhancement and the peculiarities of the phase of light. We show that properly designed plasmonic metamaterials exhibit topologically protected zero reflection yielding to sharp phase changes nearby, which can be employed to radically improve the sensitivity of detectors based on plasmon resonances. By using reversible hydrogenation of graphene[8] and binding of streptavidin–biotin[9], we demonstrate an areal mass sensitivity at a level of fg mm^{-2} and detection of individual biomolecules, respectively. Our proof-of-concept results offer a route towards simple and scalable single-molecule label-free biosensing technologies.

It is known that the phase of light exhibits non-trivial behaviour: it is a cyclic variable which is not defined at any point where the light intensity is zero (a point of complete darkness) and, as a result, shows extremely fast changes where the light intensity becomes small. Darkness can be achieved by using multiple beam interference[5], beams of higher transverse order[10] or near-fields[7]. For many applications, however, non-trivial behaviour of the light phase in the spatial frequency domain (forming the basis of Fourier optics) is required. Prominent examples of such applications include high-precision metrology and sensing, in which sharp phase features are employed to control the stability of certain characteristics or the course of processes and reactions[11]. We demonstrate below that darkness and extremely fast phase changes can be achieved by using plasmonic nanostructures (Fig. 1) and we employ this feature to improve the raw sensitivity of bio and chemical nanosensors based on optical transduction.

Optical transduction methods avoid expensive, time-consuming and precision-interfering labelling steps to mark analytes. Instead, they register the attachment of a ligand to its receptor via refractive index monitoring, which enables a real-time control of binding/recognition events[12–14]. Surface plasmon resonance (SPR) forms the core of label-free optical transduction technology, offering far superior sensitivity owing to the strong electric field probing the target molecules under conditions of resonant excitation of plasmons[15]. The spectacular progress of the SPR technology in recent years has been strongly accelerated by the development of numerous affinity models and protocols for gold surfaces. An extension of SPR, called localized plasmon resonance (LPR), is realized by using metallic nanostructures[16], which makes possible a number of new functionalities, including compatibility with modern bio-molecular nano-architectures[12], size selectivity and spectral tunability[9,16,17], strong field enhancement[18] and nano-tweezing[19].

The advances in plasmonic nanosensor technology towards the detection of trace amounts of analytes with low molecular weight (drugs, toxins and so on), such that only a few binding events are detected, is an appealing goal that could have a large impact in many fields of biomedicine, pharmacology and environmental safety[12,13]. To achieve this goal, plasmonic technology needs a drastic improvement in sensitivity. Although the existing LPR methods can detect 100–1,000 molecules of relatively large analytes[16,17], the detection limit for a 'simple' measuring scheme in terms of the amount of a biomaterial accumulated on the surface is, typically, ~1,000 pg mm^{-2}, that is, much larger than for conventional SPR (1 pg mm^{-2}; ref. 15), which in turn is inferior by 3–4 orders of magnitude to labelling methods[12]. Ultimately, the low sensitivity of plasmonic transducers is due to inherent losses in metallic nanostructures. It is worth noting that one can improve the sensitivity of a 'simple' sensing approach by using various fitting and averaging procedures, as was demonstrated for amplitude SPR (ref. 20) and LPR (ref. 21). In principle, the improvement can be significant (~1,000 times[21], see Supplementary Information) providing an additional tool for an enhancement of sensor performance in all geometries. Here, however, we discuss methods that guarantee high raw sensitivity of LPR measurements in a 'simple' optical transduction scheme. (A 'simple' optical scheme implies detection of changes of the intensity or phase of the light reflected from/transmitted through a simple plasmonic system in the case where the angle of incidence and/or light wavelength are fixed.)

The plasmonic structures suggested in this work take advantage of the enhanced phase sensitivity which occurs when the light intensity drops sharply[22]. This behaviour has already been used to improve microscopy[23] and lower the detection limit of the SPR sensing technology by at least an order of magnitude[11,24]. By designing metamaterials with diffractive coupling of localized plasmon resonances (DCLPR), (theoretically suggested in refs 25,26, first observed in ref. 27 and independently confirmed in refs 28,29) we solve the problem of inherent losses and create complete darkness,

[1]School of Physics and Astronomy, University of Manchester, Manchester M13 9PL, UK, [2]Laboratoire Lasers, Plasmas et Procédés Photoniques (LP3, UMR 7341 CNRS), Faculté des Sciences de Luminy, Aix-Marseille University, 163 Avenue de Luminy, 13288 Marseille Cedex 09, France.
*e-mail: kabashin@lp3.univ-mrs.fr; sasha@manchester.ac.uk.

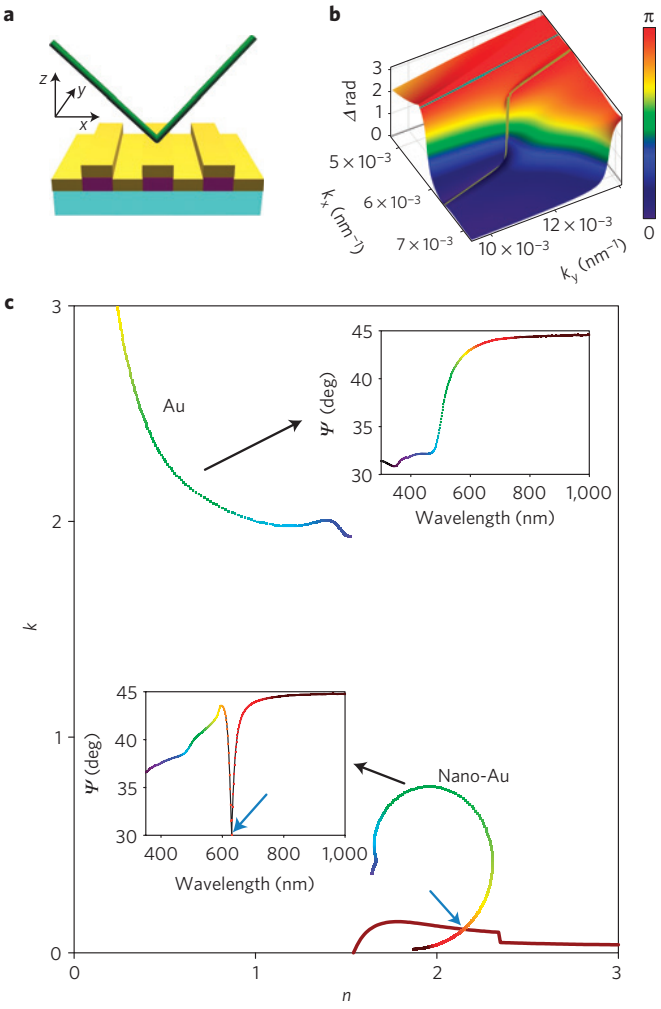

Figure 1 | Singular phase and topologically protected darkness. **a**, Schematics of light reflection from nanostructured film. **b**, Phase, Δ, of *p*-polarized light for the structure shown in **a** as a function of wave vector calculated with the effective medium theory for $\theta = 60°$, array constant $a = 320$ nm, PMMA stripes width 165 nm, gold and PMMA height 90 nm. The blue line shows smooth phase behaviour away from zero reflection, the yellow line shows the phase jump. **c**, The brown dispersion curve ($n(\lambda)$, $k(\lambda)$) corresponds to the line of zero reflection (phase singularity) for *p*-polarized light calculated with Fresnel coefficients for a 170 nm film on a glass substrate, $\theta = 60°$. The top inset shows the measured ellipsometric parameter Ψ for a 170 nm Au film, which does not exhibit any darkness. For nanostructured gold, the dispersion curve can pass through the brown curve and the reflection reaches exactly zero (provided the angle of incidence is selected in such a way that the spectral positions of intersection of the zero reflection curve and the dispersion curve coincide). The bottom curve plots the dispersion for the nanostructure (**a**) and the bottom inset shows the experimental behaviour of Ψ for the fabricated nanostructure, which exhibits topologically protected zero reflection. Blue arrows indicate intersection of the brown curve with the nano-Au curve and the sharp dip in reflection.

close to which the DCLPR demonstrate extremely high phase sensitivity. By using graphene hydrogenation, we estimate the detection limit of our metamaterials to be at the level of ≈ 0.1 fg mm^{-2} in a simple measurement scheme, which is four orders of magnitude better than reported in the literature for SPR. We also show that the suggested nanostructures can be applied to biosensing and provide an unprecedented sensitivity in the absence of labels, without any additional fitting and averaging procedures.

Our devices consist of a regular array of submicron-scale structures made from Au (Figs 1a and 2). They exhibit LPR in the visible spectrum. When light illuminates such arrays in the reflection or attenuated total reflection geometry, diffracted rays can be produced. The periodicity of our arrays is chosen in such a way that at a certain wavelength and incident angle a diffracted ray becomes grazing and couples the LPR of individual nanostructures[27], see Supplementary Information. This leads to a narrow collective plasmonic resonance[27] which is very sensitive to the environment[30], including binding events. Using diffractive coupled plasmons one can achieve an effective optical response that is not normally achievable in natural materials.

We applied coupled LPR to realize topologically protected darkness. Consider a light reflection from a thin film placed on a dielectric substrate. In the visible range, there exists a set of n, k (here $\hat{n} = n + ik$ is the refractive index of the film) for which the reflection is exactly zero, near which one would expect to have high phase sensitivity[22,30]. This set is shown by the solid brown curve in Fig. 1c. In principle, it is possible to achieve these values of n and k by using a dielectric film at an incidence angle close to the Brewster angle. Although the enhanced phase sensitivity near the Brewster angle is used in Brewster angle microscopy[23] (and ellipsometry, in general), it is not widely used in biosensing as the local electric fields for dielectric substrates are small. On the other hand, metal films can generate much stronger local fields due to plasmons and, therefore, could provide a better sensitivity. Unfortunately, it is quite difficult to achieve darkness using a continuous metal film. For example, the dispersion relations $n(\lambda)$, $k(\lambda)$ for gold yield the curve shown at the top of Fig. 1c and result in non-zero reflection for gold films across the entire visible spectrum (the measured ellipsometric reflection from a 170 nm gold film is shown in the top inset of Fig. 1c).

The situation is different for a nanomaterial with DCLPR. By using such plasmonic metamaterials, one can manipulate the effective $n_{\text{eff}}(\lambda)$, $k_{\text{eff}}(\lambda)$ and make them intersect the zero reflection line in Fig. 1c. For example, in Fig. 1 we consider gold nanostripes which are produced by depositing gold (yellow colour, thickness 90 nm) onto a poly(methyl methacrylate; PMMA) stripe array (purple colour, thickness 90 nm), although similar results can be obtained with other nanostructured metamaterials (Supplementary Information). Figure 1c shows the effective dispersion curve and the measured reflection from the gold nanostripe structure of Fig. 1a[31]. (The optical constants[31] are calculated within effective medium theory and hence could deviate from effective optical constants extracted from experiments. However, the following considerations are still valid owing to topological arguments.) One can see a narrow plasmon resonance with a half-width of ≈ 12 nm and quality factor $Q \sim 200$. A detailed analysis (see Supplementary Information) shows that the light intensity reaches zero at a certain wavelength and angle of incidence, which results in a singular behaviour of the phase in Fourier space. Indeed, the zero reflection line (the brown curve) separates two different regions in the (n, k) plane owing to the nature of Fresnel reflection coefficients. Because the dispersion curve for the nanostructured gold starts in one of these two regions and finishes in the other, it implies that it will always intersect the line of the zero reflection curve as a result of the Jordan theorem[32] (which states that the line connecting two different regions separated by a boundary always intersects the boundary), Fig. 1c. Relatively small imperfections or variations in the structure (or relatively small perturbations of the effective optical constants evaluated using different methods) will not change the fact that the dispersion curve for the nanostructured gold will connect two different regions in the (n, k) plane and hence the zero reflection for an altered structure will be still observed albeit at a slightly different wavelength. Therefore, the point of zero reflection for our metamaterial is topologically protected owing to the Jordan curve theorem. We will refer to this point as topological darkness.

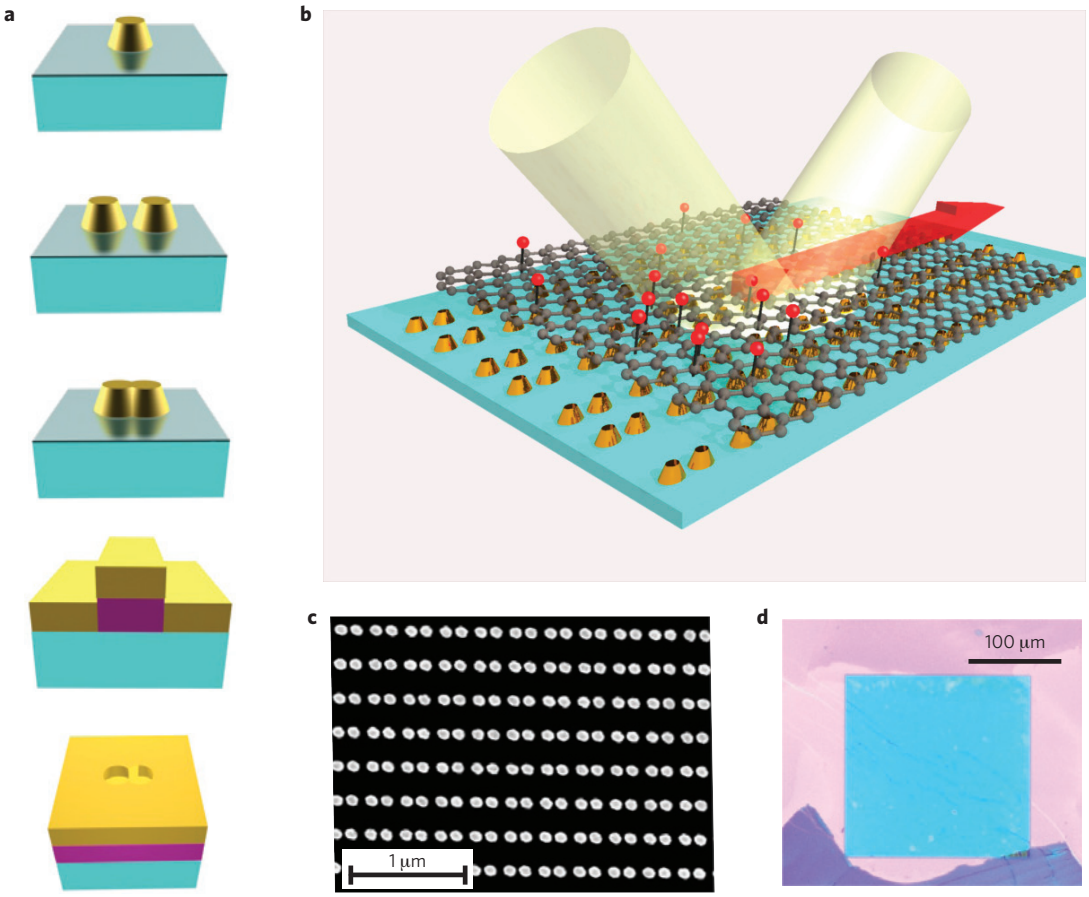

Figure 2 | Hydrogenation of graphene placed on top of a singular-phase nanostructure. a, Unit cells of various arrays that exhibited zero reflection and phase singularities in our experiments (see main text for details). **b**, Schematically, a square array of Au double-dots on a glass substrate covered by a weakly hydrogenated graphene crystal. Light beams are shown by yellow cylinders, red spheres represent hydrogen. Localized plasmon resonances of the Au dots are coupled by the grazing diffracted wave (the red arrow). **c**,**d**, A scanning electron micrograph (**c**) and optical image (**d**) of such a nanostructure.

Different excitation conditions require different structures to achieve topological darkness. Figure 2a shows a variety of unit cells for periodic nanostructures that we have experimentally employed to observe topological darkness in Fourier space (zero reflection at certain angles and wavelengths), see Supplementary Information for details. These include: nanodots (dot diameter ~100 nm, thickness ~90 nm, array period ~300 nm), double dots (which allow better control of the resonance position), gold dumbbells, stripes and arrays of holes in PMMA-gold double layers.

For sensing applications, one cannot directly use the topological darkness, owing to the absence of light and extreme jumps of phase, and should, therefore, work close to it at a point of non-complete darkness, which can be easily achieved, for example, by a slight change of angle of incidence. As we have shown in ref. 30, the ratio of phase sensitivity improvement over amplitude one can be found as $1/\Psi_{\min}$, where $\Psi_{\min}$ is the ellipsometric parameter of reflection in the resonance minimum, see Supplementary Information. Hence, choosing system parameters close to the point of topological darkness allows one to achieve the increased phase sensitivity of affinity plasmonic sensors as discussed in refs 11,22,24,30 and Supplementary Information.

To evaluate the sensitivity of the suggested plasmonic structures to chemicals adsorbed on the surface, we employed hydrogenation of graphene[8], Fig. 2b. Graphene was chosen as a test object because of a possibility to independently find the absorbed areal mass density of hydrogen using Raman spectroscopy. In addition, because graphene is easily functionalized we envisage that it may become a material of choice for calibration of plasmonic bio and chemical sensors. In our experiment, we used a $200 \times 200\ \mu m^2$ array of double dots (Fig. 2c). A graphene crystal of size $300 \times 500\ \mu m^2$ was then transferred on top of the array (Fig. 2d), which was designed in such a way that the narrow diffractive coupled resonance and close to zero reflection occurred at 603 nm at an angle of incidence ~69° (Fig. 3a). After the graphene transfer, we observed a red shift of the collective resonance to 612 nm, as shown in Fig. 3a, due to the optical properties of graphene. Figure 3b plots changes in reflection due to the graphene hydrogenation in the vicinity of the collective resonance. The inset in Fig. 3b shows the evolution of the reflection minimum (related to changes in graphene's conductivity due to hydrogenation[8]) and the resonant wavelength (due to a change of the refractive index induced by adding hydrogen atoms). It is clear that the optical properties of DCLPR are strongly affected by the graphene hydrogenation. Figure 3c shows the amplitude ratio of the D to G peaks in Raman spectra of graphene after different exposure times to atomic hydrogen. We have used this ratio to evaluate the percentage of chemically bonded hydrogen atoms to carbon atoms. For example, the ratio was ~1% after the first exposure (see ref. 8 and Methods).

To perform phase sensitive measurements, we detuned from the point of complete darkness by changing the angle of incidence θ to ensure sufficient light intensity at the resonance minimum. Figure 3d shows our most important experimental result, a change of the ellipsometric parameters, the amplitude Ψ and the phase Δ, in the vicinity of the collective resonance after the hydrogenation exposure (close to the point of 'non-complete' darkness at wavelength ~610 nm and $\theta = 70°$). One can see that the phase

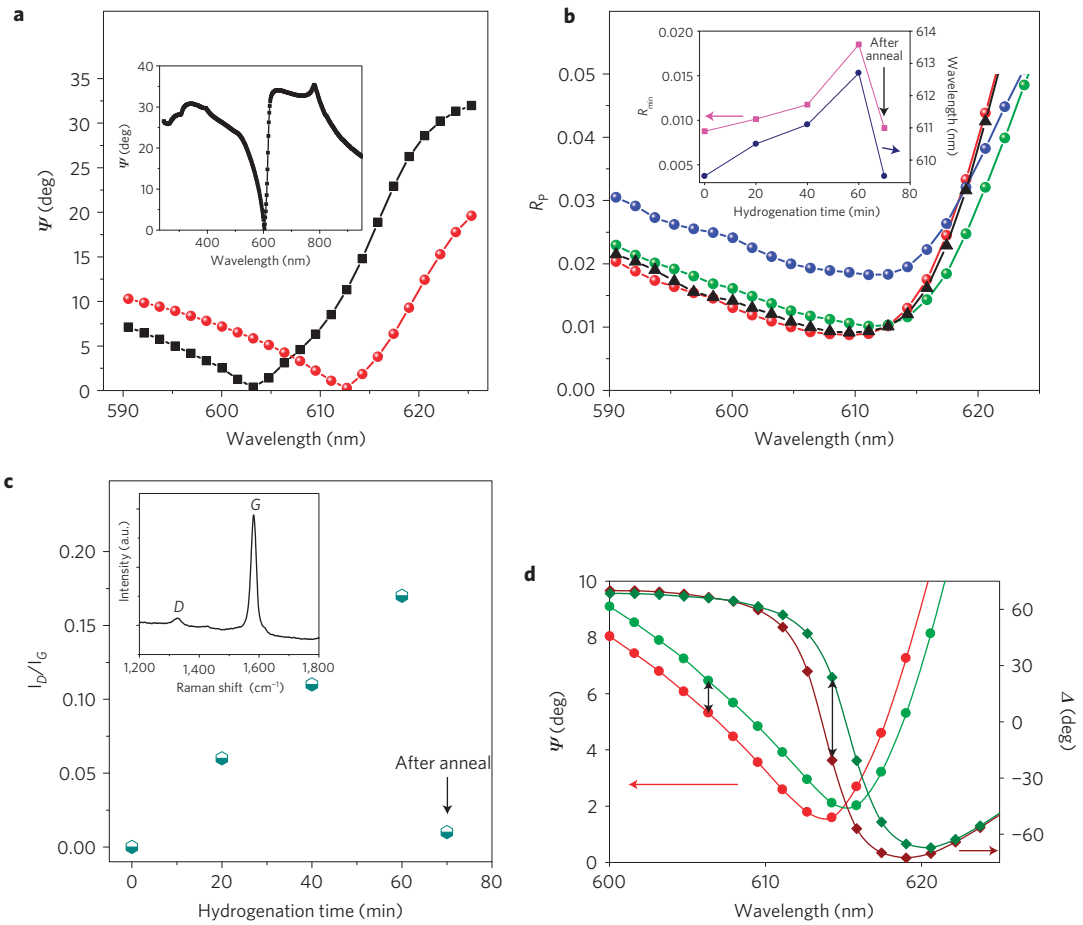

Figure 3 | Evaluation of sensitivity for singular-phase plasmonic detectors with the help of graphene hydrogenation. a, Ellipsometric reflection spectra Ψ in the region of the collective plasmon resonance for the pristine double-dot array (black curve) and with graphene transferred on top (red). The angle of incidence is 69°, the array constant $a = 320$ nm, the average size of the dots $d = 110$ nm and their separation $s = 140$ nm. The inset shows the entire spectrum for the pristine case. **b**, Evolution of the *p*-polarized reflection of the structure in **a** during hydrogenation and annealing of graphene: the red curve corresponds to initial spectra; green, 20 min of hydrogenation; blue, 60 min; black, after annealing. Inset: changes in position (right axis) and depth (left axis) of the resonance. **c**, The intensity ratio of the *D* to *G* peaks in graphene as a function of hydrogenation. The inset shows a typical Raman spectra (40 min of hydrogenation; the excitation wavelength $\lambda_{exc} = 514$ nm). **d**, Ellipsometric parameters Ψ (bright curves) and Δ (dark curves) for the cases of weakly hydrogenated (20 min, green curves) and pristine graphene (red curves) as a function of λ (incident angle of 70°).

changes by ≈44° (which is much larger than the associated relative change in Ψ). This change corresponds to a 1% hydrogen areal coverage, which translates to a mass density of $<1\,\mathrm{pg\,mm^{-2}}$. The measured phase noise level for the experimental geometry was ∼0.5°, which gives an experimental areal mass sensitivity of $<10\,\mathrm{fg\,mm^{-2}}$. If the optical system is thermally stabilized and advanced phase extraction methods are employed, a realistically achievable limit for phase noise could be as low as 5×10^{-3}deg (ref. 11). In this case, the areal mass sensitivity could reach better that $100\,\mathrm{ag\,mm^{-2}}$. It is important to note that the hydrogenation was reversible, and all the reflection and Raman spectra returned to their original form after annealing (Fig. 3b,c).

To assess the applicability of our technique to biosensing, we used a well-developed and calibrated protocol based on the streptavidin–biotin affinity model[16] (Fig. 4). The surface of a nanodot plasmonic structure was functionalized by carboxylate groups and biotin was attached to carboxylate binding sites according to the procedure described in Methods, yielding the attachment of up to 100 biotin molecules per nanodot. Finally, the biotin-covered nanodots were exposed to 10 pM streptavidin solutions in 10 mM phosphate-buffered saline for 3 h, which resulted in their binding to all the biotin sites. As shown in Fig. 4b,c, the attachment of streptavidin led to changes in the phase of reflected light by ∼25° at a light wavelength of 710 nm and angle of incidence of 53° (at the resonance minimum which corresponds to 'non-complete darkness' close to the point of topological darkness). Note that this phase shift corresponds to the attachment of 20–100 streptavidin molecules per nanodot (see Methods), which yields an experimental sensitivity of 1–4 molecules per nanodot. As was demonstrated in ref. 11, the resolution of phase measurements for a thermally stabilized system with advanced phase detection can be better than 5×10^{-3} deg, which means that in principle one could resolve the attachment of 0.004–0.02 streptavidin molecules per nanodot or <1 molecule attached per square micrometre area of our nanostructured devices. This detection limit is 2–3 orders of magnitude better than previously achieved for conventional plasmonic nanosensors based on light intensity rather than phase changes[17].

The areal mass sensitivity limit observed in graphene hydrogenation (∼$0.1\,\mathrm{fg\,mm^{-2}}$) and in biosensing (∼$1\,\mathrm{fg\,mm^{-2}}$) compares extremely well with the detection limit for LPR in simple plasmonic nanostructures (∼$1{,}000\,\mathrm{pg\,mm^{-2}}$; ref. 17, standard SPR techniques (∼$1\,\mathrm{pg\,mm^{-2}}$; ref. 15) and whispering gallery mode techniques capable of label-free single molecule detection (∼$30\,\mathrm{fg\,mm^{-2}}$; ref. 14). It is worth noting that the spot size of our optical measurements was ∼30 μm, which implies that ∼10^4

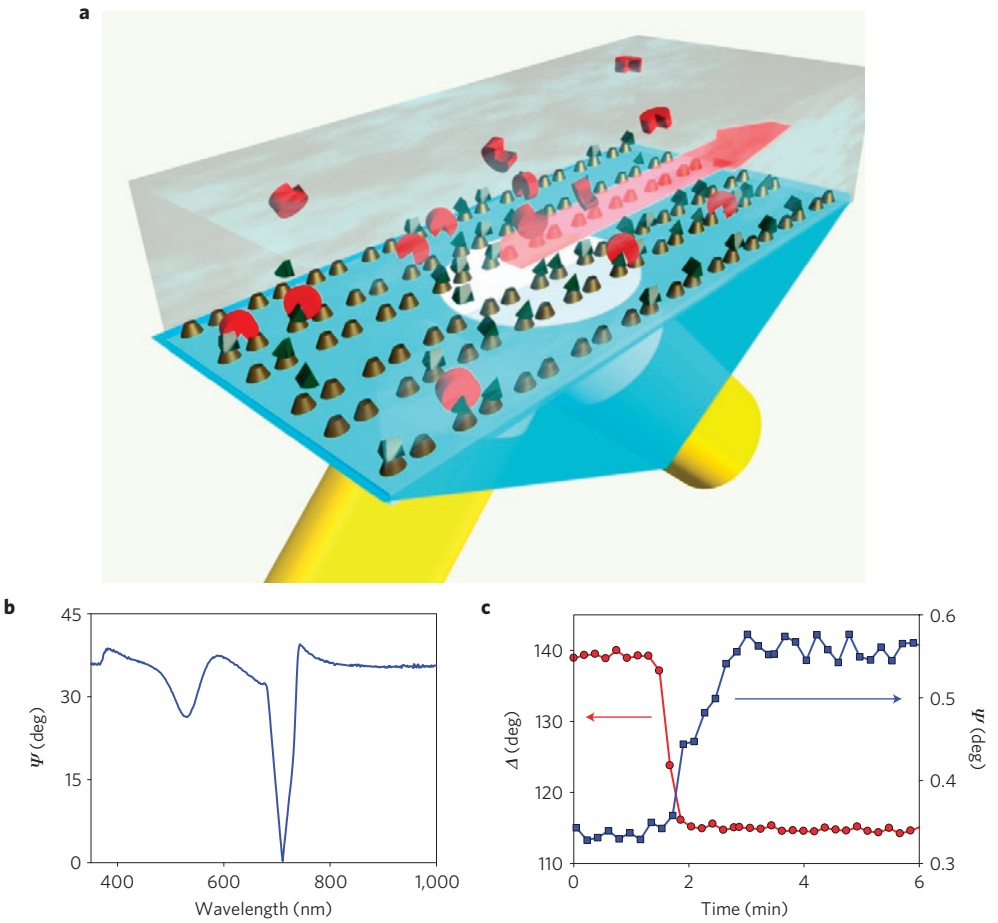

Figure 4 | Biosensing with a plasmonic metamaterial. a, Typical schematics of measurements. The dark green triangles represent biotin, the red disks represent streptavidin. Light beams are shown by yellow, the grazing diffracted wave is shown by the red arrow. The double dot array used in biosensing experiments has the following parameters: array constant $a = 320$ nm, average size of the dots $d = 135$ nm and dot separation of the pair $s = 140$ nm. **b**, Ψ versus wavelength for an incidence angle of 53°. **c**, Evolution of Δ and Ψ with time as streptavidin molecules bind to functionalized Au dots, measured at $\lambda = 710$ nm and $\theta = 53°$.

nanostructures were interrogated in each experiment. This number can be significantly reduced. Indeed, only ~100 nanodots are needed to realize DCLPR in the visible range with a quality factor $Q \sim 100$ (see Supplementary Information), which would correspond to a detection limit of 0.4–2 streptavidin molecules in the illuminated area of an array. The sensitivity can be easily improved using a curve fitting procedure and averaging. Hence, single molecule detection is indeed possible using our method with a thermally stabilized system having advanced phase detection.

To conclude, careful design of plasmonic metamaterials makes it possible to create topological darkness, resulting in pronounced phase singularities. Close to conditions of complete darkness (at the resonance minimum), plasmonic resonators demonstrate not only extremely sharp variations of reflected light intensity but also extremely fast phase changes, which can be useful for optical sensing. Our suggested plasmonic devices can be employed for molecular recognition and provide unrivalled sensitivity on the single-molecule level, offering an alternative to the existing bio- and chemical-sensing technologies. The reported metamaterials are suitable for high-throughput multi-sensing platforms and are compatible with surface-enhanced (fluorescence and Raman) techniques.

Methods

Sample fabrication, graphene transfer and optical measurements. High-quality regular and homogenous square arrays of gold nanoparticles were produced by e-beam lithography (LEO-RAITH) on a clean microscopic glass substrate covered by a thin Cr sublayer. A double layered resist was used to improve lift-off (80 nm of 495kD PMMA cast from a 3 wt% solution in anisole for the bottom resist layer and 50 nm of 95 kD PMMA cast from a 2 wt% solution in anisole for the top layer). After lithography we deposited 5 nm of Cr (to improve adhesion) and 80–90 nm Au by electron beam evaporation, which was followed by the lift-off procedure. The typical array size was 0.2×0.2 mm^2. The samples on a clean glass substrate were obtained from the samples fabricated on a 5 nm Cr sublayer (routinely used to avoid charging during electron beam lithography) in which the Cr sublayer has been wet-etched after the fabrication procedure.

Graphene was transferred on the top of a fabricated nanostructure using the following method. First, graphene was exfoliated separately onto a polymer stack consisting of a water-soluble layer (Mitsubishi Rayon aqua-SAVE) and PMMA, and the substrate Si was floated on the surface of a deionized water bath. Once the water-soluble polymer had dissolved, the Si substrate sank to the bottom of the bath, leaving hydrophobic PMMA floating on top. The PMMA membrane was adhered to a glass transfer slide, which was clamped onto the arm of a micromanipulator mounted on an optical microscope. Under the microscope, the graphene was precisely aligned to the target based on the array of Au nanostructures and the two were brought into contact. The graphene layer thickness was verified by Raman spectroscopy before the transfer procedure.

The ellipsometric spectra and polarized reflection spectra of the samples were measured by a focused beam M-2000F spectroscopic ellipsometer (J. A. Woollam) with a measurement spot of ~30 μm. We recorded a pair of ellipsometric parameters Ψ (ellipsometric reflection) and Δ (ellipsometric phase shift) in the wavelength range from 250 to 1,000 nm with a wavelength step of 1 nm. The parameter Ψ provides the ratio of field reflection coefficients for p and s polarizations and Δ gives the phase difference for the same coefficients such that $\tan(\Psi)\exp(i\Delta) = r_p/r_s$, where r_p and r_s are the complex field reflection coefficients for p and s polarizations respectively. In the M-2000F the phase Δ is determined through the ratio of in-phase and out-of-phase signals generated by a rotating

compensator. The typical measurement time of one ellipsometric spectra was about 5–10 s (depending on acquisition time for each spectral point).

Graphene hydrogenation. To bind hydrogen to the graphene surface we used a cold hydrogen d.c. plasma using a low-pressure (~0.1 mbar) H_2/Ar (1:10) gas mixture. The plasma was ignited between Al electrodes, ensuring the sample was at a safe distance (30 cm) from the discharge zone to avoid direct damage to the graphene lattice. We performed three plasma exposures of 20 min each, which provides a detectable level of single-sided hydrogenation[8]. The level of hydrogenation was estimated by measuring the D to G peak intensity ratio $I(D)/I(G)$ in the Raman spectrum of the hydrogenated samples (we used a Renishaw RM1000 spectrometer with a 514 nm excitation wavelength). It has been demonstrated[33] that the ratio can be used to determine the typical distance between the defects L_D using the following relation: $L_D = 4.24 \times 10^{-5}\lambda^2\sqrt{I(G)/I(D)}$, where λ is the wavelength measured in nanometres, $I(G)$ and $I(D)$ are the counts for G and D Raman peaks of hydrogenated graphene. This gives an estimate of $L_D \approx 50$ nm after the first hydrogenation. However, taking into account the tendency for hydrogen atoms to form clusters on the surface of graphene, we have to assume that L_D provides us only with the typical distance between the clusters of hydrogen atoms. To estimate the number of hydrogen atoms attached to graphene, we assume that the size of the cluster is smaller than the inter-cluster distance (5 nm), which gives us an estimate of 1% hydrogenation. To check the reversible nature of hydrogenation we annealed the sample in a nitrogen atmosphere for 4 h at 200 °C.

Biosensing experiment. We repeated the protocol described and calibrated in ref. 16. Glass slides with gold nanodots were incubated for 24 h in 1 mM of 3:1 ethanolic solution of 1-octanethiol (1-OT) and 11-mercaptoundecanoic acid (11-MUA) purchased from Sigma-Aldrich, yielding the formation of a self-assembling monolayer with a 10% surface coverage of carboxylate binding sites[16]. As the active surface of each nanodot was equal to $\sim 10^4 nm^2$, such a procedure led to 2,000 active sites per nanodot. After incubation, the nanodots were rinsed with ethanol and dried in flowing nitrogen. Then, 1 mM biotin (Sigma-Aldrich) in 10 mM Phosphate-Buffered Saline (PBS) solution was linked to surface carboxyl groups using 1-ethyl-3-[3-dimethylaminopropyl] carbodiimide hydrochloride coupling over a 3 h period. Taking into account the ~1–5% efficiency of such coupling[16], up to 20–100 biotin molecules attach to each nanodot. Finally, the biotin-covered nanodots were exposed to 10 pM streptavidin (Sigma-Aldrich) solutions in 10 mM PBS for 3 h. Samples were finally rinsed with 10 mM PBS and water to remove all non-specifically bound molecules.

Received 4 April 2012; accepted 30 November 2012; published online 13 January 2013

References

1. Aharonov, Y. & Bohm, D. Significance of electromagnetic potentials in the quantum theory. *Phys. Rev.* **115,** 485–491 (1959).
2. Berry, M. V. Quantal phase factors accompanying adiabatic changes. *Proc. R. Soc. Lond. A. Math. Phys. Sci.* **392,** 45–57 (1984).
3. Allen, L., Padgett, M. J., Babiker, M. & Wolf, E. *Progress in Optics* Vol. 39, 291–372 (Elsevier, 1999).
4. Molina-Terriza, G., Torres, J. P. & Torner, L. Twisted photons. *Nature Phys.* **3,** 305–310 (2007).
5. Dennis, M. R., King, R. P., Jack, B., O'Holleran, K. & Padgett, M. J. Isolated optical vortex knots. *Nature Phys.* **6,** 118–121 (2010).
6. Nye, J. F. & Berry, M. V. Dislocations in wave trains. *Proc. R. Soc. Lond. A. Math. Phys. Sci.* **336,** 165–190 (1974).
7. Yu, N. *et al.* Light propagation with phase discontinuities: Generalized laws of reflection and refraction. *Science* **334,** 333–337 (2011).
8. Elias, D. C. *et al.* Control of graphene's properties by reversible hydrogenation: Evidence for graphane. *Science* **323,** 610–613 (2009).
9. Kabashin, A. V. *et al.* Plasmonic nanorod metamaterials for biosensing. *Nature Mater.* **8,** 867–871 (2009).
10. Allen, L., Beijersbergen, M. W., Spreeuw, R. J. & Woerdman, J. P. Orbital angular momentum of light and the transformation of Laguerre–Gaussian laser modes. *Phys. Rev. A* **45,** 8185–8189 (1992).
11. Kabashin, A. V., Patskovsky, S. & Grigorenko, A. N. Phase and amplitude sensitivities in surface plasmon resonance bio and chemical sensing. *Opt. Express* **17,** 21191–21204 (2009).
12. Prasad, P. N. *Introduction to Biophotonics* (Wiley, 2003).
13. Cooper, M. A. Optical biosensors in drug discovery. *Nature Rev. Drug Discov.* **1,** 515–528 (2002).
14. Vollmer, F. & Arnold, S. Whispering-gallery-mode biosensing: Label-free detection down to single molecules. *Nature Methods* **5,** 591–596 (2008).
15. Liedberg, B., Nylander, C. & Lundström, I. Biosensing with surface plasmon resonance—how it all started. *Biosensors Bioelectron.* **10,** i–ix (1995).
16. Haes, A. J. & Van Duyne, R. P. A nanoscale optical biosensor: Sensitivity and selectivity of an approach based on the localized surface plasmon resonance spectroscopy of triangular silver nanoparticles. *J. Am. Chem. Soc.* **124,** 10596–10604 (2002).
17. Anker, J. N. *et al.* Biosensing with plasmonic nanosensors. *Nature Mater.* **7,** 442–453 (2008).
18. Nie, S. & Emory, S. R. Probing single molecules and single nanoparticles by surface-enhanced Raman scattering. *Science* **275,** 1102–1106 (1997).
19. Grigorenko, A. N., Roberts, N. W., Dickinson, M. R. & Zhang, Y. Nanometric optical tweezers based on nanostructured substrates. *Nature Photon.* **2,** 365–370 (2008).
20. Johansen, K., Stålberg, R., Lundström, I. & Liedberg, B. Surface plasmon resonance: Instrumental resolution using photo diode arrays. *Meas. Sci. Technol.* **11,** 1630 (2000).
21. Dahlin, A. B., Tegenfeldt, J. O. & Höök, F. Improving the instrumental resolution of sensors based on localized surface plasmon resonance. *Anal. Chem.* **78,** 4416–4423 (2006).
22. Grigorenko, A. N., Nikitin, P. I. & Kabashin, A. V. Phase jumps and interferometric surface plasmon resonance imaging. *Appl. Phys. Lett.* **75,** 3917–3919 (1999).
23. Hoenig, D. & Moebius, D. Direct visualization of monolayers at the air–water interface by Brewster angle microscopy. *J. Phys. Chem.* **95,** 4590–4592 (1991).
24. Kabashin, A. V. & Nikitin, P. I. Interferometer based on a surface-plasmon resonance for sensor applications. *Quant. Electron.* **27,** 653–654 (1997).
25. Zou, S., Janel, N. & Schatz, G. C. Silver nanoparticle array structures that produce remarkably narrow plasmon lineshapes. *J. Chem. Phys.* **120,** 10871–10875 (2004).
26. Markel, V. A. Divergence of dipole sums and the nature of non-Lorentzian exponentially narrow resonances in one-dimensional periodic arrays of nanospheres. *J. Phys. B* **38,** L115–L121 (2005).
27. Kravets, V. G., Schedin, F. & Grigorenko, A. N. Extremely narrow plasmon resonances based on diffraction coupling of localized plasmons in arrays of metallic nanoparticles. *Phys. Rev. Lett.* **101,** 087403 (2008).
28. Auguie, B. & Barnes, W. L. Collective resonances in gold nanoparticle arrays. *Phys. Rev. Lett.* **101,** 143902 (2008).
29. Chu, Y., Schonbrun, E., Yang, T. & Crozier, K. B. Experimental observation of narrow surface plasmon resonances in gold nanoparticle arrays. *Appl. Phys. Lett.* **93,** 181108 (2008).
30. Kravets, V. G., Schedin, F., Kabashin, A. V. & Grigorenko, A. N. Sensitivity of collective plasmon modes of gold nanoresonators to local environment. *Opt. Lett.* **35,** 956–958 (2010).
31. Kravets, V. G., Schedin, F. & Grigorenko, A. N. Plasmonic blackbody: Almost complete absorption of light in nanostructured metallic coatings. *Phys. Rev. B* **78,** 205405 (2008).
32. Hales, T. C. The Jordan curve theorem, formally and informally. *Am. Math. Monthly* **114,** 882–894 (2007).
33. Canciado, L. G. *et al.* Quantifying defects in graphene via Raman spectroscopy at different excitation energies. *Nano Lett.* **11,** 3190–3196 (2011).

Acknowledgements

We are grateful to the SAIT GRO Program, European Commission (Metachem), and French National Research Agency (ANR).

Author contributions

A.N.G. and A.V.K. conceived the idea. V.G.K., F.S., R.J., R.V.G. and D.A. made the devices. V.G.K., L.B., B.T., K.S.N., A.N.G. and A.V.K. modified samples and performed measurements. All the authors contributed to discussion of the project. A.K.G., K.S.N. and A.N.G. guided the project. A.N.G., A.V.K., K.S.N. and A.K.G. wrote the manuscript with revisions from all authors.

Additional information

Supplementary information is available in the online version of the paper. Reprints and permissions information is available online at www.nature.com/reprints. Correspondence and requests for materials should be addressed to A.V.K. or A.N.G.

Competing financial interests

The authors declare no competing financial interests.